INTERLAYER SHEAR IN BILAYER GRAPHENE CRYSTALS

Guorui Wang[1,2], Luqi Liu[1*], and Zhong Zhang[1*]

[1] National Center for Nanoscience and Technology, Beijing 100190, PR China
[2] University of Science and Technology of China, Hefei 230026, PR China

Keywords: graphene; Raman spectroscopy; interlayer interaction; shear deformation; bubble.

1 INTRODUCTION

Two-dimensional (2D) materials, monolayer atoms with crystalline structures and unusual physical characteristics, have been fueling extensive research on their use in semiconductors, electronics, battery energy and composites.[1] For most exciting applications of 2D crystals, the emergence of multilayer structures is inevitable either because of the production process limitations,[2] or more importantly, because of the functional and operating requirements.[3-6] Indeed, ordered structures comprised of two or more layers represent a wide class of materials and their extraordinary properties can be modulated by taking advantage of interlayer interactions. Recently, significant developments have been achieved in recent years in characterizing mechanical properties of graphene and beyond-graphene 2D crystals.[7-10] The multilayer system was typically treated as a single sheet where the interlayer deformation is overlooked. Such treatment assumed strong interaction between layers, making the exploration on interlayer shear parameters elusive.[7-10] On the contrary, the interlayer vdW interaction creates weak points in the mechanical sense that individual layers with atom-level smooth surfaces were believed to be highly lubricated.[11,12] To date, the understanding of deformation and failure mechanisms in multilayer structures remains experimentally challenging, and the quantitative characterization of interlayer interaction has yet to emerge.

2 RESULTS AND DISCUSSIONS

To activate interlayer shear deformation in bilayer graphene system, we utilize pressure in the hole as a controlling load, forcing supported graphene (outside the hole) towards the center of hole by a controllable bulging process (Figure 1). Multi-type characterization techniques were employed including (Fig. 1a): *in situ* Raman spectroscopy to monitor interlayer shear deformation and *in situ* AFM to characterize the height profile of the bubble in efforts to explore the interlayer shear effect on the overall bugling behaviors.

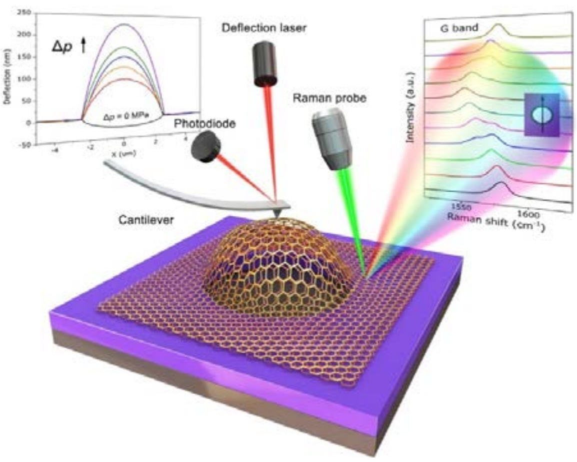

Figure 1: Schematic diagram of a bilayer graphene bulging device and its multi-type characterizations for the interlayer deformation.

Guorui Wang[1,2], Luqi Liu[1*], and Zhong Zhang[1*]

When graphene membrane is bulged upwards, a zone with strain gradient around the hole can be observed as evidenced by the Raman G-band red-shifts, which is clear indicator of interfacial shear deformation governed by interfacial shear stress, τ_1, between graphene and the substrate (Figure 2c-e). In contrast, a much more discernable growth behavior or larger shear zone is visible in bilayer samples outside the hole, which is dominated by the shear deformation at the weak graphene/graphene interface, as shown in Figure 2f-h. We parameterized by a dimensionless ρ that is the ratio between the radius of the shear zone and the radius of the hole to describe the growth of shear zone and further determined the underlying interfacial/interlayer stress with respect to our applied pressure difference. The obtained value of shear stress for graphene/SiO_2 interfaces (τ_1) is in 1-3 MPa with average of 1.64 MPa, while for graphene/graphene interfaces (τ_2) is in 0.02-0.06 MPa with average of 0.04 MPa.

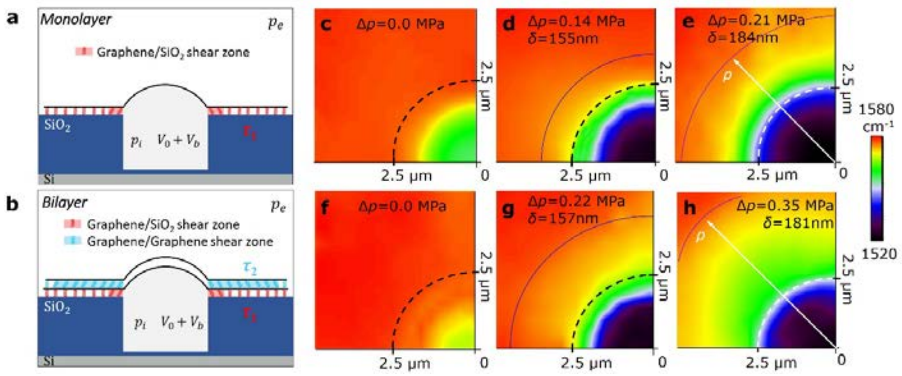

Figure 2: Schematic diagram of bulging of (a) monolayer and (b) bilayer graphene samples after removed from the pressure chamber, triggering the supported regions surrounding the hole to exhibit an inclination to slide towards the center. Raman contour maps of G band frequency in the first quadrant revealed the strain distributions as shown in (c-e) monolayer graphene system and (f-h) bilayer graphene system of both suspended and supported regions (discriminated by the dashed line) at different amplitudes of pressure. The growth of shear zones is indicated by the solid lines.

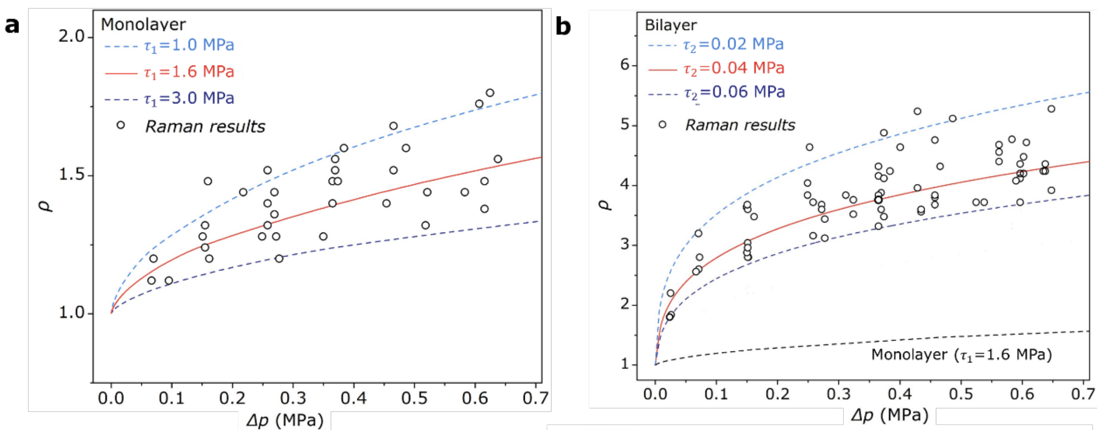

Figure 3: The growth of shear zone in graphene/SiO_2 interface versus pressure difference Δp for (a) monolayer and (b) bilayer graphene system. Circular symbols are Raman results.

3 CONCLUSIONS

Here, for the first time, we report the experimental measurement of the interlayer shear resistance in bilayer graphene and demonstrated the continuously controlled growth of interlayer shear zone via a bubble loading device. We uncover that such a process is governed by previously overlooked interlayer shear deformation, whose characteristics could be well captured by considering interlayer shear stress and strain. The governing shear resistance of 40 kPa was revealed in the bilayer interfaces. To the best of our knowledge, this is the first measurement of the interfacial shear resistance of the atomic thickness structures and it hence sheds light on a new experimental and theoretical framework to understand the interlayer shear deformations in emerging 2D materials. The capability to probe the interlayer interaction is significant for the assembly and processing of layered 2D materials and further offers a deep insight into the stacking structure-property relations.

REFERENCES

1 Geim, A. K. & Novoselov, K. S. The rise of graphene. *Nat. Mater.* **6**, 183-191 (2007).

2 Li, X. *et al.* Large-area synthesis of high-quality and uniform graphene films on copper foils. *Science* **324**, 1312-1314 (2009).

3 Ponomarenko, L. *et al.* Tunable metal-insulator transition in double-layer graphene heterostructures. *Nat. Phys.* **7**, 958-961 (2011).

4 Geim, A. K. & Grigorieva, I. V. Van der Waals heterostructures. *Nature* **499**, 419-425 (2013).

5 Bunch, J. S. *et al.* Electromechanical resonators from graphene sheets. *Science* **315**, 490-493 (2007).

6 Nair, R., Wu, H., Jayaram, P., Grigorieva, I. & Geim, A. Unimpeded permeation of water through helium-leak–tight graphene-based membranes. *Science* **335**, 442-444 (2012).

7 Bertolazzi, S., Brivio, J. & Kis, A. Stretching and breaking of ultrathin MoS2. *ACS Nano* ***5**, 9703-9709 (2011).*

8 Conley, H., Lavrik, N. V., Prasai, D. & Bolotin, K. I. Graphene bimetallic-like cantilevers: probing graphene/substrate interactions. *Nano Lett.* **11**, 4748-4752 (2011).

9 Koenig, S. P., Boddeti, N. G., Dunn, M. L. & Bunch, J. S. Ultrastrong adhesion of graphene membranes. *Nat. Nanotechnol.* **6**, 543-546 (2011).

10 Kitt, A. L. *et al.* How graphene slides: Measurement and theory of strain-dependent frictional forces between graphene and SiO2. *Nano Lett.* **13**, 2605-2610 (2013).

11 Zhang, R. *et al.* Superlubricity in centimetres-long double-walled carbon nanotubes under ambient conditions. *Nat. Nanotechnol.* **8**, 912-916 (2013).

12 Zhang, R. *et al.* Interwall Friction and Sliding Behavior of Centimeters Long Double-Walled Carbon Nanotubes. *Nano Lett.* **16**, 1367-1374 (2016).